A polysaccharide extract from the medicinal plant Maidong inhibits the IKK–NF-κB pathway and IL-1β–induced islet inflammation and increases insulin secretion

Received for publication, May 15, 2020, and in revised form, June 22, 2020 Published, Papers in Press, June 30, 2020, DOI 10.1074/jbc.RA120.014357

Dandan Mao[1], Xiao Yu Tian[2], Di Mao[3], Sze Wan Hung[3], Chi Chiu Wang[3], Clara Bik San Lau[4], Heung Man Lee[1], Chun Kwok Wong[5], Elaine Chow[1,6], Xing Ming[1], Huanyi Cao[1], Ronald C. Ma[1,7,8], Paul K. S. Chan[9], Alice P. S. Kong[1,7,8], Joshua J. X. Li[10], Guy A. Rutter[11,12], Wing Hung Tam[3], and Juliana C. N. Chan[1,7,8,*]

From the [1]Department of Medicine and Therapeutics, the [3]Department of Obstetrics and Gynaecology, the [5]Department of Chemical Pathology, the [6]Phase 1 Clinical Trial Centre, the [7]Hong Kong Institute of Diabetes and Obesity, the [8]Li Ka Shing Institute of Health Sciences, the [9]Department of Medical Microbiology, and the [10]Department of Anatomical and Cellular Pathology, Chinese University of Hong Kong, Prince of Wales Hospital, Hong Kong, China, the [2]School of Biomedical Sciences and the [4]Institute of Chinese Medicine and State Key Laboratory of Research on Bioactivities and Clinical Applications of Medicinal Plants, Chinese University of Hong Kong, Hong Kong, China, the [11]Division of Diabetes, Endocrinology, and Metabolism, Department of Metabolism, Digestion, and Reproduction, Imperial College London, London, United Kingdom, and the [12]Lee Kong Chian School of Medicine, Nan Yang Technological University, Singapore

Edited by Jeffrey E. Pessin

The herb dwarf lilyturf tuber (Maidong, *Ophiopogonis Radix*) is widely used in Chinese traditional medicine to manage diabetes and its complications. However, the role of Maidong polysaccharide extract (MPE) in pancreatic β-cell function is unclear. Here, we investigated whether MPE protects β-cell function and studied the underlying mechanisms. We treated *db/db* and high-fat diet (HFD)-induced obese mice with 800 or 400 mg/kg MPE or water for 4 weeks, followed by an oral glucose tolerance test. Pancreas and blood were collected for molecular analyses, and clonal MIN6 β-cells and primary islets from HFD-induced obese mice and normal chow diet–fed mice were used in additional analyses. *In vivo*, MPE both increased insulin secretion and reduced blood glucose in the *db/db* mice but increased only insulin secretion in the HFD-induced obese mice. MPE substantially increased the β-cell area in both models (3-fold and 2-fold, $p < 0.01$, for *db/db* and HFD mice, respectively). We observed reduced nuclear translocation of the p65 subunit of NF-κB in islets of MPE-treated db/db mice, coinciding with enhanced glucose-stimulated insulin secretion (GSIS). *In vitro*, MPE potentiated GSIS and decreased interleukin 1β (IL-1β) secretion in MIN6 β-cells. Incubation of MIN6 cells with tumor necrosis factor α (TNFα), interferon-γ, and IL-1β amplified IL-1β secretion and inhibited GSIS. These effects were partially reversed with MPE or the IκB kinase β inhibitor PS1145, coinciding with reduced activation of p65 and p-IκB in the NF-κB pathway. We conclude that MPE may have potential for therapeutic development for β-cell protection.

More than 450 million people are affected worldwide by diabetes, the majority having type 2 diabetes (T2D) (1, 2). Although there are many classes of antidiabetic drugs, Chinese medicines remain a popular remedy for diabetes in China (3). Among these remedies, dwarf lilyturf tuber (Maidong, *Ophiopogonis Radix*) is widely used, with experimental data supporting its antidiabetic effects. In OLEFT T2D rat models, Maidong improved glucose homeostasis, inhibited abdominal fat accumulation, and enhanced hepatic glucose uptake (4). In diabetic mice, Maidong fractions delayed carbohydrate digestion and absorption with improvement of lipid metabolism (5, 6). One of the Maidong (MDG-1) monosaccharide molecules attenuated insulin resistance through the phosphatidylinositol 3-kinase/protein kinase B pathway in diabetic mice (7, 8). In this light, α-glucosidase inhibitors (such as acarbose), proven not only to prevent but also cause remission of diabetes, also have a complex polysaccharide structure (9). Maidong demonstrated a cardioprotective effect by attenuating profibrotic signals, including thrombospondin 1 and transforming growth factor β (10). However, the effects of Maidong on pancreatic β-cell function remain unknown. Insulin resistance, mainly mediated through obesity and inflammation, as well as insulin insufficiency contribute to the development of T2D, with β-cell dysfunction being particularly relevant in Asians (11). Factors that contribute to β-cell dysfunction include but are not limited to glucolipotoxicity, inflammation, and endoplasmic reticulum stress (12, 13), alongside genetic predisposition (14). In experimental conditions, glucolipotoxicity activates inflammatory signals such as nuclear factor-κB (NF-κB), interleukin-1β (IL-1β), IL-6, interferon-γ (IFN-γ), and tumor necrosis factor α (TNFα), which impair insulin secretion (13). IL-1β can activate the NF-κB signaling cascade followed by Fas dysregulation and DNA fragmentation, resulting in β-cell dysfunction (15). IFN-γ or TNFα can activate the c-Jun N-terminal kinase and protein kinase C pathways to impair β-cell function (16). Of note, β-cells are the main cells within the islets that release IL-1β in response to elevated glucose. This effect can exacerbate hyperglycemia by causing further β-cell dysfunction (17). In support of this view, treatment of diabetic animals and human

This article contains supporting information.

* For correspondence: Juliana C. N. Chan, jchan@cuhk.edu.hk.
Present address for Juliana C. N. Chan: Dept. of Medicine and Therapeutics, Chinese University of Hong Kong, Prince of Wales Hospital, Hong Kong, China.

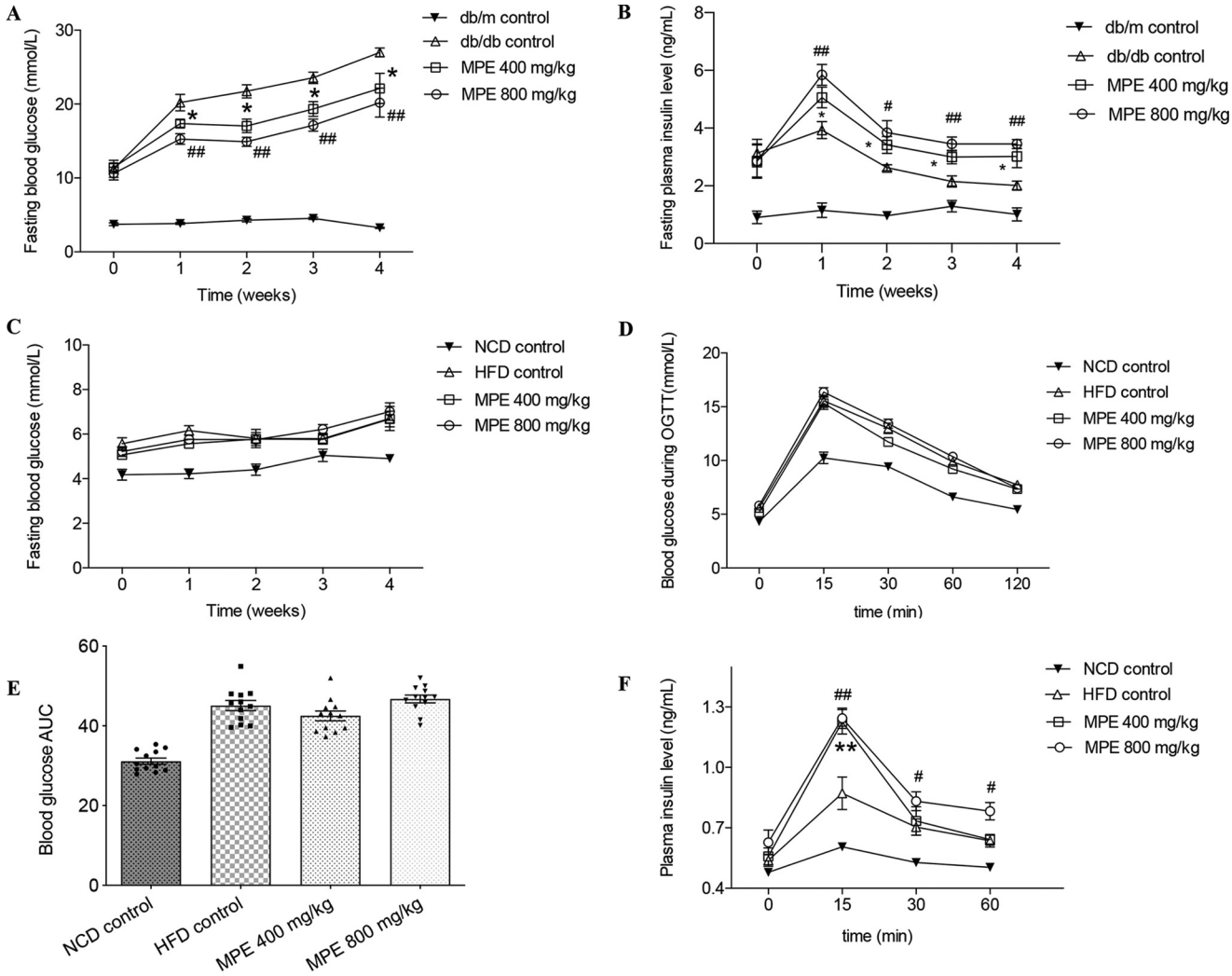

Figure 1. MPE reduces blood glucose in *db/db* mice and maintains blood glucose in HFD-induced obese mice by increasing insulin secretion. *A* and *B*, results from *db/db* mice; *C–F*, results from HFD-induced obese mice. *A* and *B*, weekly fasting blood glucose levels (*A*) and insulin levels (*B*) in *db/db* mice treated with 400 mg/kg MPE, 800 mg/kg MPE, or control after 4 weeks of force-feeding. *C*, weekly fasting blood glucose levels in HFD-induced obese mice treated with 400 mg/kg MPE, 800 mg/kg MPE, or control after 4 weeks of force-feeding. *D*, OGTT (glucose at 1 g/kg body weight) after 4 weeks of treatment with MPE and control in HFD-induced obese mice. *E* and *F*, AUC of blood glucose during OGTT (*E*) and plasma insulin levels measured at different time points during OGTT (*F*) in HFD-induced obese mice. Data are presented as mean ± S.E. (*error bars*) with individual data points in the histogram (*db/db* mice: $n = 7$; HFD-induced obese mice: $n = 8$). #, 800 mg/kg MPE *versus db/db* control; *, 400 mg/kg MPE *versus db/db* control. # or *, $p < 0.05$; ## or **, $p < 0.01$.

pancreatic islets with IL-1β receptor antagonist has been shown to improve insulin production and glycemic control with preservation of β-cell mass and function (15, 18–20).

Polysaccharides from many Chinese herbs, such as *Curcuma longa*, *Morinda citrifolia* Linn, and *Wedelia chinensis*, are found to have beneficial effects in a broad spectrum of diseases, such as inflammatory bowel disease and extremity and ear infections. These beneficial effects are mediated through various mechanisms, including reduced production of inflammatory cytokines and inhibition of leukocytes migration (21–23). Against this background, we selected IL-1β as a possible target to explore the antidiabetic effect of MPE. We hypothesized that MPE might lower blood glucose by reducing inflammation in β-cells and thus increasing insulin secretion. To test this hypothesis, we used multiple, complementary *in vivo* and *ex vivo* models. First, *db/db* mice and high-fat diet (HFD)-induced obese mice were used to examine the antidiabetic effect of MPE *in vivo*. Next, we used clonal MIN6 β-cells (24) to explore changes in gene expressions *in vitro* by microarray analysis. MIN6 cells and primary islets from HFD-induced obese mice and C57 BL6/J mice were also used to examine the expression and release of inflammatory markers.

Results

MPE attenuated blood glucose in db/db mice and maintained blood glucose in HFD-induced obese mice by increasing insulin secretion

Treatment of *db/db* mice for 4 weeks with MPE at 400 or 800 mg/kg or with water as a control reduced fasting blood glucose levels in a dose-dependent manner. At week 4, fasting blood glucose increased from a mean ± SEM of 10 ± 0.49 mmol/litre to 20.2 ± 1.1 mmol/liter in the control group, compared with 17.3 ± 0.5 mmol/liter in the MPE 400 mg/kg group ($p < 0.05$) and 15.3 ± 0.7 mmol/liter in the MPE 800 mg/kg group ($p < 0.01$) (Fig. 1*A*). There was no further reduction in blood glucose

during the oral glucose tolerance test (OGTT) (Fig. S2*D*) or insulin tolerance test (ITT) in both treatment groups (Fig. S2*C*). Peak insulin secretion was 5.06 ± 0.36 ng/ml in the 400 mg/kg group and 5.84 ± 0.36 ng/ml in the 800 mg/kg group, both of which were significantly higher than that in the control group (3.93 ± 0.29 ng/ml) (Fig. 1*B*). There was no effect of MPE on body weight, food intake, lipid, or GLP-1 levels (Figs. S1–S4).

Area under the curve (AUC) of blood glucose were increased during OGTT and ITT after 10 weeks of HFD feeding compared with normal chow diet (NCD) mice (Fig. S3). After MPE treatment, there was no difference in fasting blood glucose levels between the two groups (Fig. 1*B*). Treatment with MPE did not change blood glucose (Fig. 1, *D* and *F*) but enhanced glucose-stimulated insulin secretion (GSIS) during OGTT in HFD-induced obese mice compared with control mice ($p < 0.01$) (Fig. 1*H*).

MPE treatment led to an increase in the percentage of pancreatic area occupied by β-cells in both db/db mice and HFD-induced obese mice

After treatment for 4 weeks, pancreata were isolated from both mouse models for staining of glucagon and insulin. Fig. 2 (*A* and *B*) shows representative images of glucagon, insulin, and DAPI in each group of *db/db* mice and HFD-induced obese mice, respectively. In both *db/db* mice and HFD-induced obese mice, the β-cell areas, as a percentage of the overall pancreatic section, increased substantially (3- and 2-fold, respectively) and significantly after treatment with either dose of MPE (Fig. 2, *C* and *D*) compared with the control group. There was no change in α-cell areas with MPE in either model (Fig. 2, *E* and *F*).

MPE increased GSIS and high glucose–impaired ATP/ADP ratio in MIN6 cells and primary islets isolated from HFD-induced obese mice

We used MIN6 cells as an *in vitro* cellular model with GSIS and ATP/ADP ratio as indicators of β-cell function and viability. We treated MIN6 cells with vehicle or MPE at concentrations of 0.05, 0.5, 5, and 50 μg/ml for 24, 48, and 72 h, followed by measurements of GSIS and high glucose–induced ATP/ADP ratio. Insulin secretion did not change after MPE treatment (0.5 μg/ml) for 24 and 48 h (Fig. 3, *A* and *B*) but increased at 72 h (MPE *versus* control: 0.38 ± 0.02 *versus* 0.28 ± 0.02 ng/μg of protein, $p < 0.05$) (Fig. 3*A*). Treatment with MPE (0.5 μg/ml) increased the ATP/ADP ratio in MIN6 cells (MPE *versus* control: 6.30 ± 0.94 *versus* 1.51 ± 0.11, $p < 0.01$) (Fig. 3*B*). In primary islets isolated from HFD-induced obese mice, MPE (0.5 μg/ml) treatment for 72 h induced a robust increase in both GSIS (MPE *versus* control: 247.2 ± 35.80 *versus* 117.6 ± 9.01 ng/μg of protein, $p < 0.01$) (Fig. 3*C*) and ATP/ADP ratio (Fig. 3*D*) (MPE *versus* control: 0.72 ± 0.07 *versus* 0.49 ± 0.03, $p < 0.05$).

MPE decreased islet p65 nuclear translocation in db/db mice but did not affect cellular proliferation in HFD-induced obese mice

We applied microarray analysis to MIN6 cells to explore the underlying mechanism with and without MPE treatment. The RNA expressions of *il1β* and *nf*κb1 were reduced after treatment with MPE (0.5 μg/ml) (Fig. 4). *In vivo*, MPE reduced p65 nuclear translocation in islets of *db/db* mice (Fig. 5, *A* and *B*). In addition, MPE also reduced the expression of IL-1β in islets from both animal models (Fig. S4).

In vitro, expression of IL-1β in MIN6 cells and primary islets was down-regulated by MPE treatment (0.5 μg/ml). After inflammatory cytokine challenge, IL-1β production induced by IL-1β or a cytokine mixture (IL-1β + TNFα + IFNγ) was attenuated with MPE treatment (0.5 μg/ml) compared with cells untreated with MPE (Fig. 5). We subtracted the amount of exogenous IL-1β (20 ng/ml in single challenge, 10 ng/ml in mixture challenge) to measure the endogenous secretion.

To determine whether cytokine production was involved in β-cell dysfunction and was modulated by MPE, we performed GSIS in primary islets from NCD mice treated with the inflammatory cytokines above. As shown in Fig. 5*G*, MPE did not exert any effect on islets from NCD mice under low-glucose conditions. Both IL-1β and the cytokine mixture inhibited insulin secretion, and these effects were attenuated by the addition of MPE (0.5 μg/ml). At the same time, MPE increased insulin secretion treated with IL-1β and the cytokine mixture. Furthermore, in primary islets from NCD mice *in vitro*, MPE reduced levels of mRNA encoding *il1b* (Fig. 5*H*) induced by IL-1β alone or the cytokine mixture. MPE also decreased the production of IL-1β in MIN6 cells and primary islets from HFD-induced obese mice. However, MPE did not increase cellular proliferation in islets of HFD-induced obese mice (Fig. S5).

MPE inhibited pro-inflammatory IκB kinase (IKK) signaling under hyperglycemia in β-cells

IL-1β, upon binding with its receptor, can activate the MyD88–IKKβ–NF-κB pathway to increase expression of *il1b* to further impair β-cell function (20). To test the potential effects of MPE on this pathway, we used MIN6 cells cultured in low-glucose (5.5 mmol/liter) or high-glucose (25 mmol/liter) medium for 72 h and treated with or without MPE. Treatment was followed by measurement of GSIS, ATP/ADP ratio, and IL-1β production. As shown in Fig. 6, pretreatment with high glucose impaired insulin secretion and reduced ATP/ADP ratio, accompanied by up-regulation of IL-1β at both the mRNA and protein levels. In Fig. 6 (*A* and *B*), treatment of MIN6 cells with IKK inhibitor (PS1145, 5 μmol/liter) in high glucose attenuated the apparent inflammatory response and improved β-cell function. This was accompanied by increased GSIS and high glucose–induced ATP/ADP ratio in MIN6 cells. When co-administered with MPE, PS1145 blocked the improvements in insulin secretion and ATP/ADP ratio achieved by MPE. In the control group treated with a high concentration (20 ng/ml) of IL-1β, the addition of PS1145 tended to increase insulin secretion and ATP/ADP ratio by blocking the intrinsic production of IL-1β (Fig. 6, *A* and *B*). In MIN6 cells treated with MPE, PS1145 reversed the reduction of IL-1β by MPE with increased RNA expression and protein level of IL-1β (Fig. 6, *C* and *D*).

Incubation of MIN6 or islet cells in high-glucose medium increased phosphorylation of the NF-κB subunit p65 and IκB,

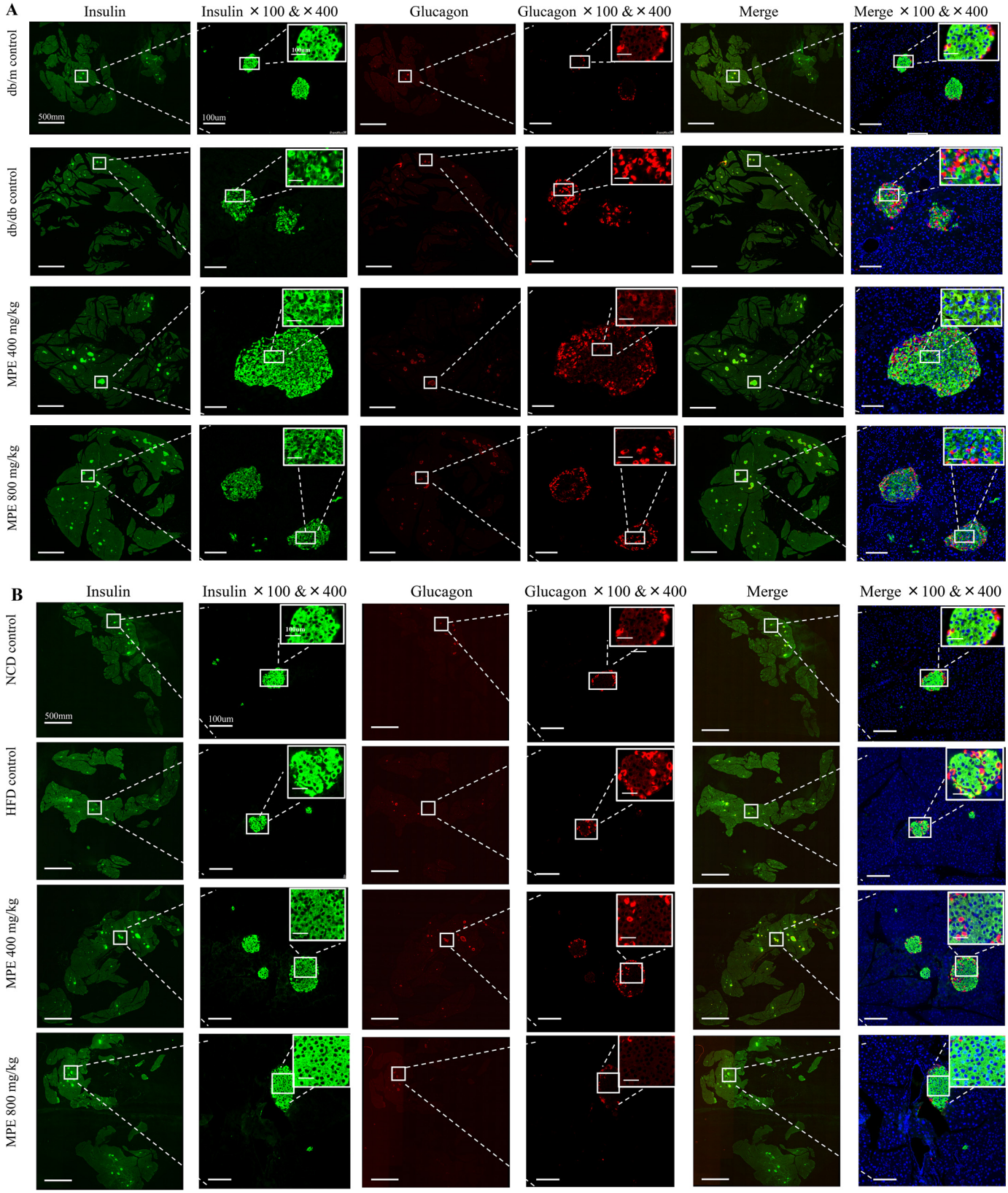

Figure 2. MPE increases the percentage of pancreatic area occupied by β-cells in *db/db* mice and HFD-induced obese mice. *A* and *B*, immunofluorescence staining of insulin and glucagon in the pancreas of *db/db* mice (*A*) and HFD-induced obese mice (*B*) (*green*, insulin; *red*, glucagon; *blue*, DAPI). Images in the *first*, *third*, and *fifth columns* represent the total pancreatic area in each slide of each group. *White scale bar*, 500 mm. The *second*, *fourth*, and *sixth columns* represent *zoom-out islets* in the selected area of the total pancreatic area in the magnification of ×100 and ×400. The latter is presented in the *top right corner*. *White scale bar*, 100 μm. *C* and *E*, relative quantification of glucagon-positive α-cells in *db/db* mice (*C*) and HFD-induced obese mice (*E*) by ImageJ software ($n = 5$ in each group). Relative quantification of insulin-positive β-cells in *db/db* mice (*D*) and HFD-induced obese mice (*F*) by ImageJ software ($n = 5$ in each group). Data are presented as mean ± S.E. (*error bars*) with individual data points in histograms. *, $p < 0.05$; **, $p < 0.01$.

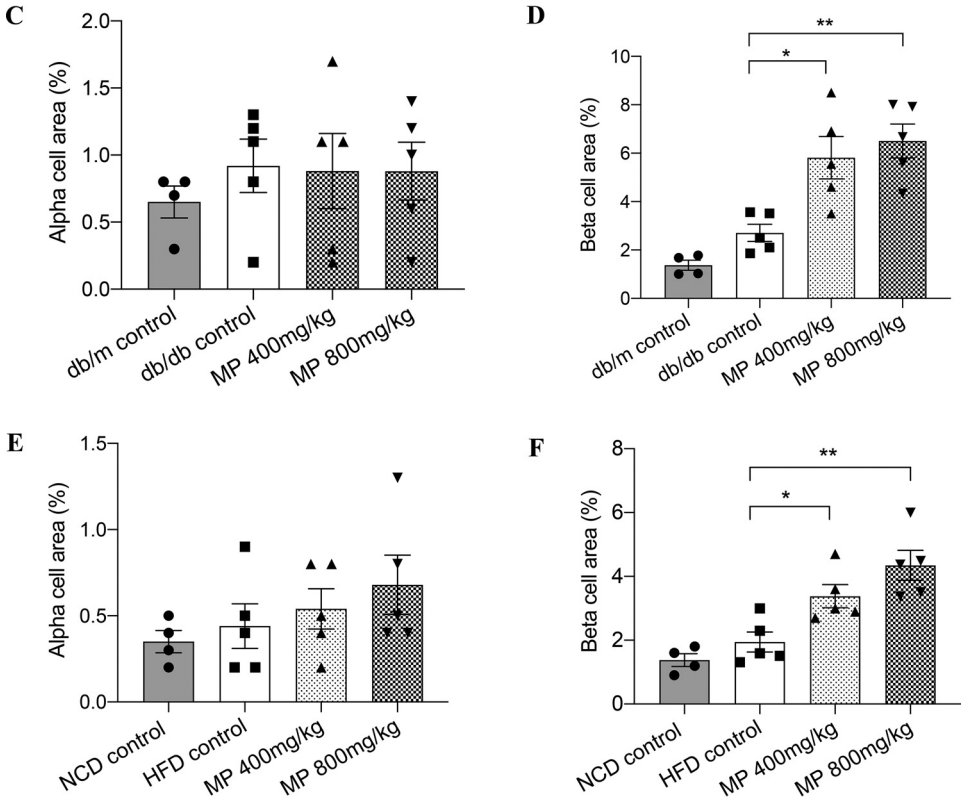

Figure 2 —*continued*

indicating NF-κB activation. Treatment with MPE decreased p65 and IκB phosphorylation in MIN6 cells compatible with reduced activation of NF-κB (Fig. 7). Similarly, MPE reduced p65 and IκB phosphorylation in primary islets from HFD-induced obese mice (Fig. 7, *D–F*).

In primary islets from NCD mice, IL-1β alone or the cytokine mixture increased phospho-p65 (p-p65) and phospho-IκB (p-IκB) levels, as shown in Fig. 7 (*G–I*). Pretreatment with MPE inhibited the increase of phosphorylation of both p65 and IκB. However, MPE did not totally eliminate the inhibitory effects of multiple cytokines on islet function, suggesting possible roles for other signaling pathways (*e.g.* protein kinase C, mitogen-activated protein kinase, signal transducer and activator of transcription 1, etc. (25)).

Discussion and conclusions

In this study, we used two *in vivo* models and two *in vitro* models to evaluate the effects of MPE. MPE increased insulin secretion in both mice models and reduced blood glucose in *db/db* mice. A summary of the major effects of MPE in the five different systems is provided in Table 1 and is discussed in more detail below.

Microarray analysis revealed that MPE treatment decreased the levels of mRNAs encoding several genes, including *pik3ca, pik3cd* (phosphatidylinositol-4,5-bisphosphate 3-kinase catalytic subunit α/δ), *csf2* (colony-stimulating factor 2), *nfκb1* (Fig. 4, *G–J*), and *il1β* (Fig. 5*C*) in MIN6 cells. *pik3ca* and *pik3cd* are protein-coding genes in the family of phosphoinositide 3-kinases. They play an essential role in the insulin signal transduction pathway via the activation of the Akt/protein kinase B to regulate glucagon synthesis, glucose, and lipid metabolism (26). As mentioned in the Introduction, MPE has been reported to reduce insulin resistance in diabetic animal models. Another gene, *csf2*, is a white blood cell growth factor that stimulates stem cells to produce granulocyte and monocyte, although an impact on glucose homeostasis is less clear in this case.

In the present study, we focused on *il1b* as an important target gene because IL-1β is an essential inflammatory cytokine involved in β-cell dysfunction. Furthermore, in randomized clinical trials, IL-1β antagonist has been shown to restore β-cell dysfunction in patients with T2D (20). In support of these human data, treatment with MPE reduced RNA expression of *il1β* and *nfκb1* in MIN6 cells. The production of IL-1β is induced by IKK–NF-κB–mediated transcription (27, 28) through p65 nuclear translocation. MPE decreased p65 nuclear translocation in islets of *db/db* mice, indicative of reduced islet inflammation induced by IL-1β. Consequently, it seems reasonable to conclude that reduced inflammation contributes to the increase of the percentage of pancreatic area occupied by β-cells and hence enhanced insulin secretion after MPE treatment.

We chose HFD-induced obese mice as a model to examine cellular proliferation after MPE treatment rather than *db/db* mice. Given the milder glycemic phenotype, we suspected that the HFD-induced obese mouse model was more likely than *db/db* mice to have residual β-cells with a greater capacity for regeneration in response to treatment with MPE (Fig. S3, *A* and *B*). Nevertheless, we found that MPE did not affect islet cellular proliferation detected by BrdU staining in HFD-induced obese mice (Fig. S5). The expansion of β-cell area is

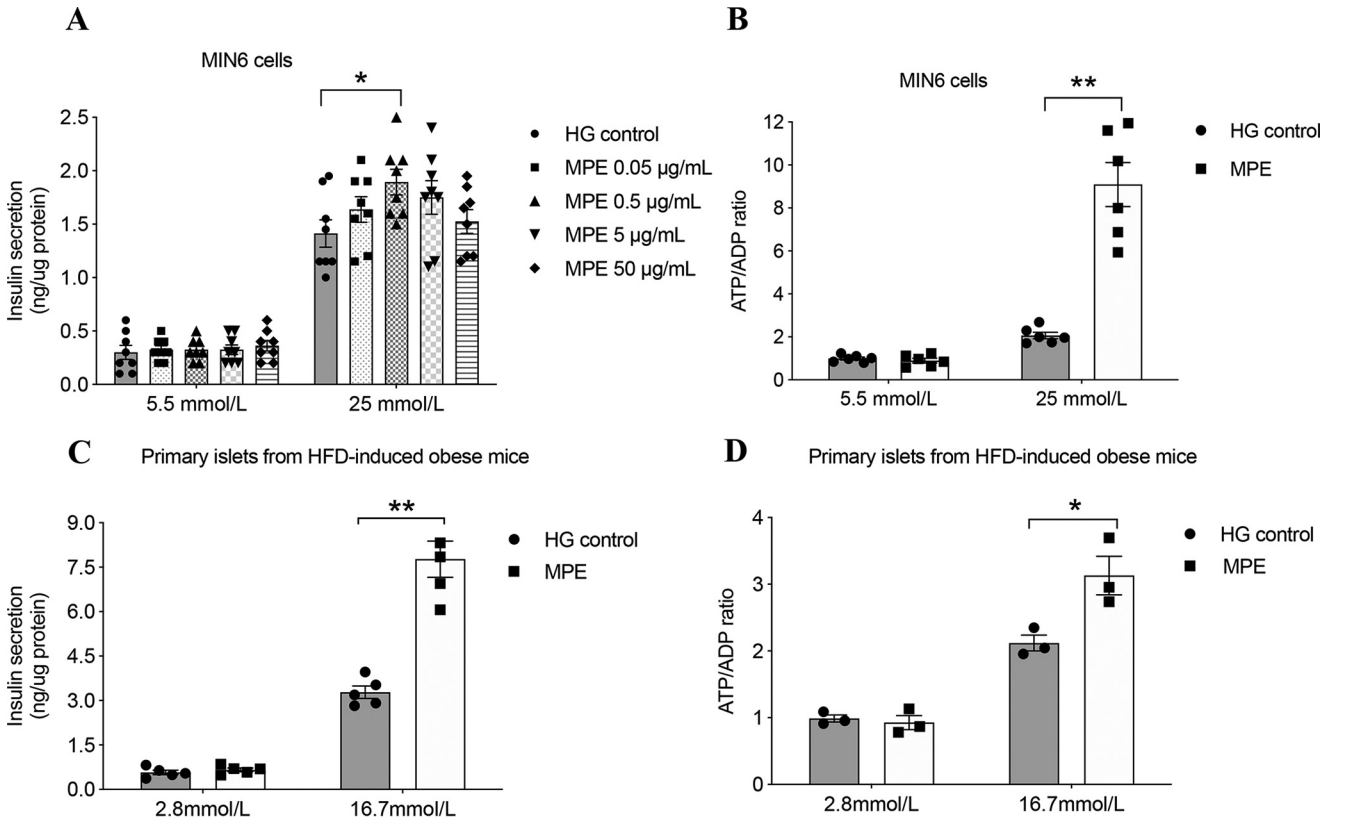

Figure 3. MPE increases ATP/ADP ratio and improves GSIS. *A*, GSIS was performed to evaluate the secretory function of MIN6 cells following treatment with control or MPE (0.05, 0.5, 5, and 50 μg/ml) for 72 h. HG control represents high-glucose medium (25 mmol/liter) without MPE. *B*, ATP/ADP ratio was measured during GSIS in MIN6 cells. *C*, GSIS was performed to evaluate the secretory function of primary islets from HFD-induced obese mice following treatment with control or MPE (0.5 μg/ml) for 72 h. *D*, ATP/ADP ratio was measured during GSIS in primary islets of HFD-induced obese mice. Data are presented as mean ± S.E. (*error bars*) with individual data points in histograms. *, $p < 0.05$; **, $p < 0.01$.

regulated by several mechanisms, including β-cell neogenesis with differentiation from precursor cells, β-cell proliferation with an increase in cell number, and β-cell hypertrophy with an increase in cell size (12, 29). Because MPE does not affect cell proliferation, the expansion of β-cell area might be due to differentiation or cell hypertrophy, which will require exploration in future studies. Apart from cell proliferation, we also examined apoptosis in HFD-induced obese mice using a TUNEL assay, but we did not find identifiable apoptosis-positive signals in the islets with or without MPE treatment (Fig. S6). Taken together, our data suggest that MPE treatment enhances insulin secretion largely by suppressing NF-κB–mediated IL-1β transcription in pancreatic islets with the expansion of β-cell area.

In MIN6 cells and primary islets from HFD-induced obese mice and C57 mice, MPE treatment with or without inflammatory cytokines reduced IL-1β secretion and improved GSIS and ATP/ADP ratio (Fig. 5, *C–H*). Further molecular analysis confirmed that MPE reduced the expression of phosphorylated IκB and p65 in both islets and MIN6 cells. In MIN6 cells, this effect was reversed by PS1145, an IKK inhibitor. MPE treatment with IKK inhibitor did not improve insulin secretion and caused an increase in IL-1β expression in MIN6 cells (Fig. 6). These findings suggest that MPE might compete with IKK inhibitor in this IKK–IκB–NF-κB pathway for a site of action. However, there is no relevant literature on PS1145 to indicate whether it is an irreversible or reversible inhibitor. More pharmacological assays, including enzyme kinetics, velocity, and pharmacodynamics, will be necessary in the future to fully understand the pharmacological action(s) of MPE.

We used HFD-induced obese mice as a model of insulin resistance. In these euglycemic animals, we only demonstrated the insulin-enhancing (Fig. 1*F*), and not the anti-hyperglycemic, effect of MPE (Fig. 1*C*). On the other hand, in *db/db* diabetic mice, MPE exhibited significant anti-hyperglycemic effects (Fig. 1*A*). Despite the insulin secretion–enhancing effect of MPE, we did not observe hypoglycemia or weight gain in either animal model.

In the present experiments, the anti-inflammatory effect of MPE was dose- and time-dependent with 0.5 μg/ml for 72 h having the most optimal effects in MIN6 cells and islets. MPE with higher doses of 5 and 50 μg/ml did not show any improvement in GSIS. This is probably due to the high molecular weight of MPE in high concentration, which may inhibit its entry into the cytoplasm.

Given the close links between glucotoxicity and β-cell dysfunction, any measures that ameliorate glucotoxicity are expected to improve β-cell function and/or survival. Several Chinese herbs can attenuate insulin resistance (30) with secondary effects on β-cell function. As discussed previously, MPE has been proven to delay carbohydrate absorption and improve lipid metabolism, whereas a fraction of MPE has been shown to

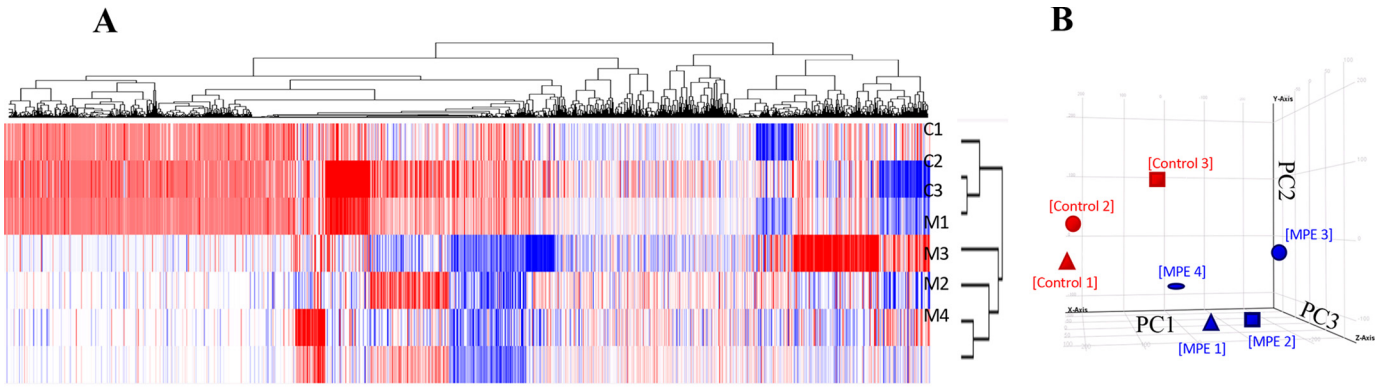

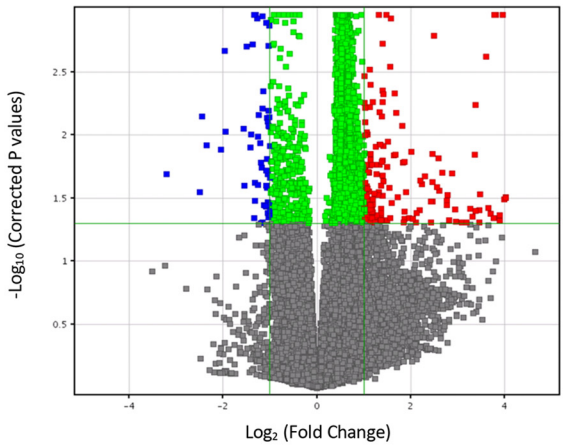

D

Pathway	P value
Inflammatory Response Pathway	0
Protein-protein interactions in the podocyte	1.88E-09
Chemokine signaling pathway	8.50E-09
Senescence and Autophagy	1.59E-08
Spinal Cord Injury	3.23E-07
Toll-like receptor signaling pathway	3.92E-06
PluriNetWork	5.21E-05
Nicotine degradation II	6.05E-05
Cytokines and Inflammatory Response	2.15E-04
TLR	4.16E-04
Bupropion degradation	4.41E-04
Nicotine degradation III	8.39E-04
Phosphate acquisition II	0.002614
Regulation of Actin Cytoskeleton	0.004805
Myometrial Relaxation and Contraction Pathways	0.005392
MAPK signaling pathway	0.005514
MicroRNAs in cardiomyocyte hypertrophy	0.006096
Apoptosis	0.006304
Parathion degradation	0.008969
Neural Crest Differentiation	0.009665
TFs Regulate miRNAs related to cardiac hypertrophy	0.017858
Insulin Signaling	0.034162
miRNA regulation of DNA Damage Response	0.034733

Figure 4. Gene expression microarray and pathway analysis shows significant inhibition of IL-1β–IKK–NF-κB pathway by MPE treatment. *A*, *k*-means clustering; *B*, principal component analysis. Gene expression profiles of MPE-treated MIN6 cells are grouped together. The *x* axis shows principal component 1 (PC1), the *y* axis shows PC2, and the *z* axis shows PC3. *C*, volcano plot. Differential up-regulated and down-regulated genes are identified. *D*, gene ontology analysis. Chemokine, cytokine, inflammatory, TLR, and insulin pathways are major pathways in the differentially expressed genes. *E*, heat map. Differential down-regulated genes cluster in MPE-treated MIN6 cells are shown. Relative gene expression levels and -fold changes of *pik3cd*, *tlr6* (Toll-like receptor 6), *nfkb1*, *cd40*, *pik3ca*, and *il1b* are shown. *Red*, up-regulations in control samples; *blue*, down-regulations in MPE-treated samples. *F*, MPE treatment attenuated the inflammatory IL-1β–IKK–NF-κB pathway. *Red labels* indicate the significant down-regulated genes in the pathway. *G–J*, validation of expression of *pik3ca*, *pik3cd*, *nfkb1*, and *csf2* by RT-PCR. *Error bars*, S.E.

improve insulin resistance (6). However, due to differences in extraction methods and compositions of MPE, the MPE used in our experiments did not demonstrate any effect on attenuating insulin resistance.

Using a reductionist approach to identify specific active molecules in a Chinese medicine often fails to explain the benefits of the original herb or its multicomponent extracts (31). In this context, we have reported the effects of multicomponent herbal medicine in altering multiple pathways to reverse fatty liver with remission of diabetes in animal models (31) and accelerate the healing of diabetic ulcers in human studies (32). Other researchers (33–35) have also demonstrated that some plant-based remedies contain natural prodrugs that are chromatin modifiers, such as resveratrol and harmine, which have been shown to preserve islet structure and improve β-cell biology. Given the complex nature of typical Chinese medicines, these multitargeted effects are not unexpected and may help restore homeostasis with potential for both prevention and treatment of diabetes.

There are limitations in our study. In particular, more in-depth investigations are needed to evaluate the causal nature of the antidiabetic effects of MPE via amelioration of the IL-1β signaling pathway. This will require molecular studies to confirm the role of IL-1β in insulin secretion and modulating effects of MPE in such experimental models. Pending these experiments, the antidiabetic effects of IL-1β receptor antagonist in human clinical trials (20) provide some corroborative evidence in support of our experimental results.

We demonstrated that MPE did not improve the lipid profile in HFD-induced obese mice (Fig. S7). Treatment with MPE also did not improve β-cell function impaired by palmitate-induced lipotoxicity (Fig. S8). We did not examine the effects of MPE on oxidative stress, other inflammatory signals or cell cycles, or cross-talk between macrophages and islet. It is likely

E

Genes	Control 1	Control 2	Control 3	MPE1	MPE2	MPE3	MPE4	fold changes	p values
Pik3cd	0.549825	1.901103	1.329274	-0.06563	-0.02174	0	-0.42519	-2.6175342	0.003046
Tlr6	0	0.698301	0.965592	-1.83131	-0.07448	-0.57073	-0.15544	-2.2585263	0.028153
Nfkb1	1.36674	0.056613	0.966953	0	-0.64965	-0.28387	-0.78562	-2.0660517	0.030241
Cd40	0	0.329111	0.476909	-1.19446	-1.57989	-0.41051	-0.12752	-2.0462832	0.03255
Pik3ca	0	1.614955	0.977544	-0.24821	-0.52076	-0.32445	-0.29861	-1.9342741	0.0441
Il1b	0.321607	0.637959	0.488076	-0.39795	0	-0.01382	-0.45982	-1.6250069	0.046149

2.0 1.5 1.0 0.5 0.0 -0.5 -1.0 -1.5 -2.0

F

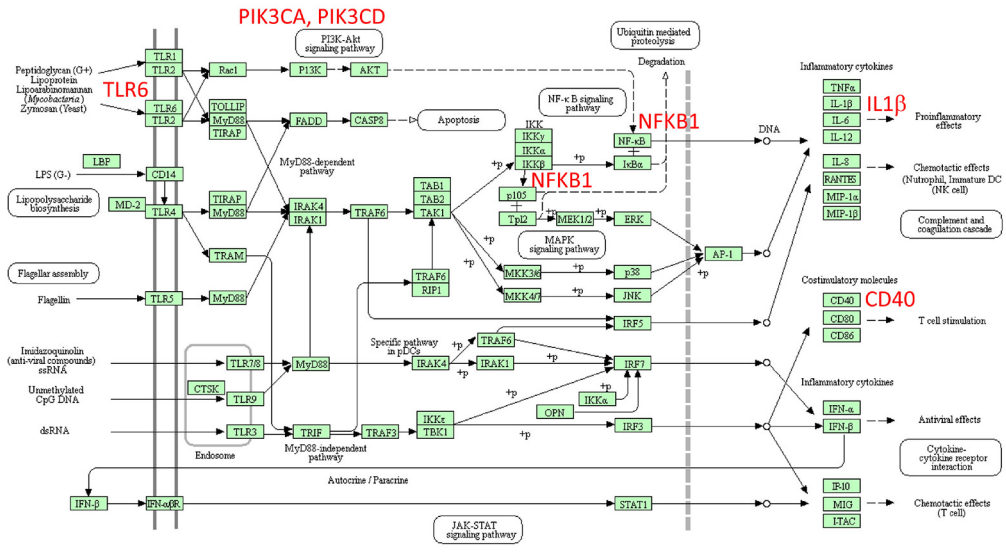

G

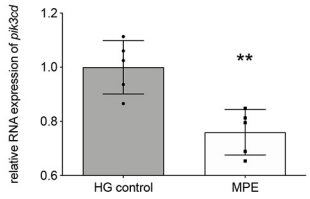

H

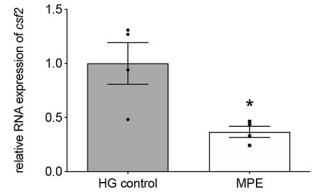

I

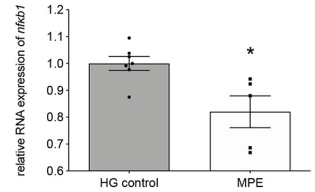

J

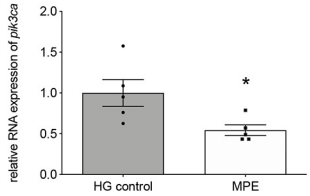

Figure 4 —*continued*

that many monosaccharides and proteins in the MPE complex may work in concert to exert a therapeutic effect. However, due to the large molecular size of MPE, the mechanisms involved in MPE entry into the β-cell and its effects on other intracellular functions, such as mitochondrial metabolism and protein trafficking, or mediators, such as circulating noncoding RNA, require further elucidation (36).

Despite these limitations, our data allow us to conclude that the ameliorating effects of MPE on hyperglycemia and cytokine-induced loss of β-cells and their dysfunction are likely mediated through inhibition of the IL-1β–IKK–NF-κB pathways. Whereas future studies will be required to identify the active component(s) within the MPE that mediates these different effects, our results highlight the potential of developing Chinese medicines for prevention and early treatment of diabetes.

Materials and methods

Maidong polysaccharide preparation

The fresh roots of *Ophiopogonis Radix* (Zhixin Medicine Ltd., Hong Kong, sample 131101) were crushed and boiled in water at 100 °C for 1 h. After collecting the water extract, we added freshwater to the boiler for the second time and boiled for 1 h. The water extract from the two boiling treatments was mixed, filtered, and concentrated by a Rotavapor R-220 (BUCHI). The concentrated Maidong solution was added in a ratio of 1:5 (v/v) to 95% ethanol for overnight precipitation. The precipitates were dissolved in distilled water, followed by centrifugation to improve purity following the aforementioned water extraction processes repeated twice. The final precipitates were dissolved in distilled water and underwent lyophilization to form a white power for use in these experiments and was referred to as Maidong polysaccharide extract (MPE).

Total carbohydrate percentage and molecular weight of MPE were 91.96% and 3.72 kDa, respectively, measured by the colorimetric method with phenol-sulfuric acid and gel permeation chromatography, respectively. Amino acid and monosaccharide composition are shown in Fig. S1. Of note, arginine, glutamine, and asparagine **a**re the top three amino acids whose deficiencies are associated with impaired glucose metabolism and increased risk of diabetes (37–39). In the present study, we used the entire fraction of MPE because a single monosaccharide, amino acid, or other constituent is unlikely to mediate all of the complex biological effects of this extract.

The dosage of Maidong whole-water extract was 6-12 g/60 kg of body weight in the Chinese Pharmacopoeia. For mice, the dosage of MPE was calculated using the equation, mouse dose (mg/kg) = human dose (mg/kg) × K_m ratio (9.01) based on a previous report (40), which yielded a dose of 0.9 mg/kg. The weight ratio of MPE was 23% of the whole extract, and we used 200 and 400 mg/kg MPE as equivalent to 1 and 2 clinical doses, respectively.

Animal experiments, oral glucose tolerance test, insulin tolerance test

All experimental procedures were approved by the Animal Experimentation Ethics Committee of the Chinese University of Hong Kong (CUHK). Female *db/db* mice (Jackson Stock no.

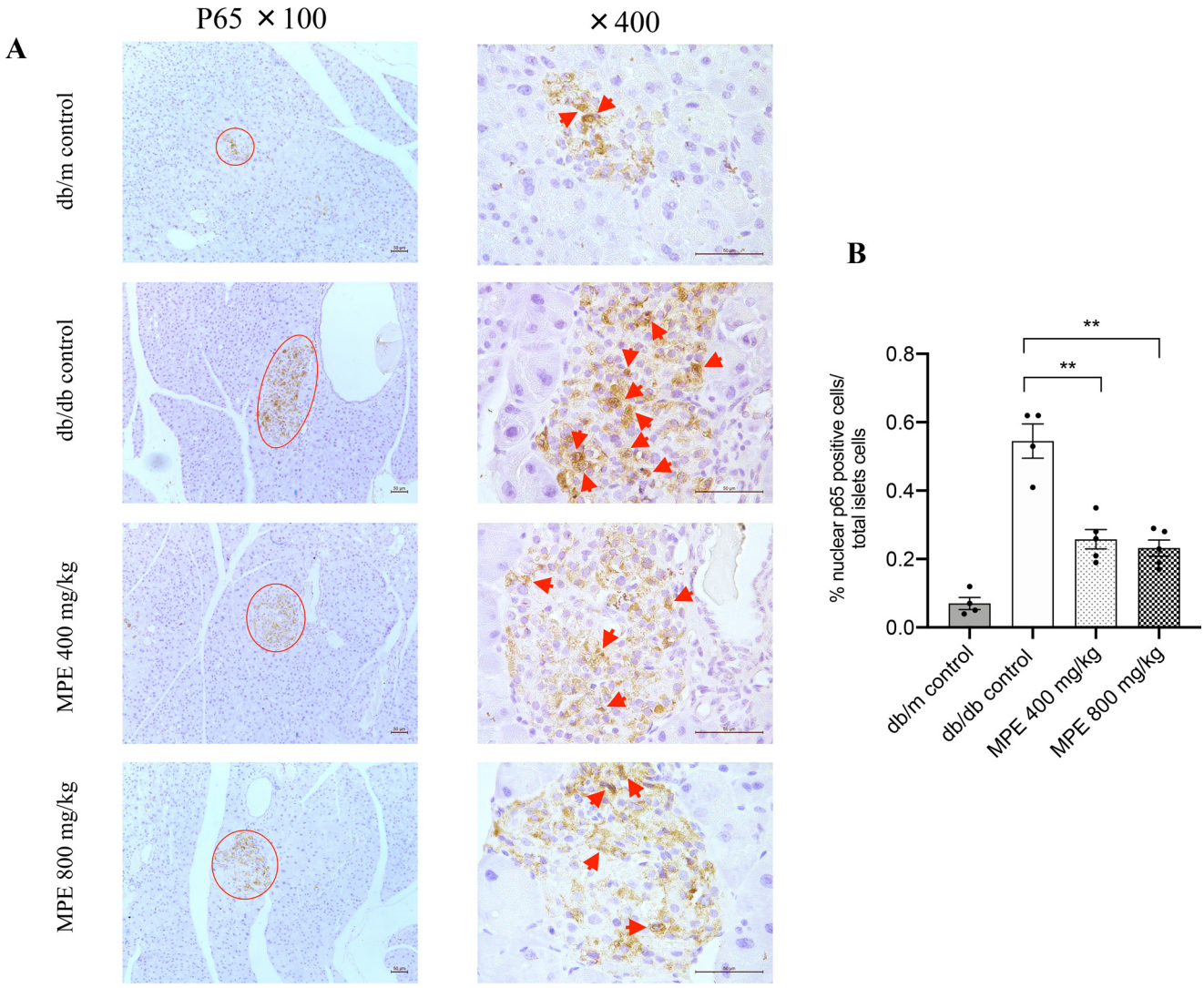

Figure 5. Impact of MPE on NF-κB p65 nuclear staining and IL-1β expression. *A*, immunohistochemistry staining of p65 in the nucleus of pancreas of *db/db* mice (magnification: ×100 and ×400; both the *short* and *long black scale bars* in the *top panel* in the *bottom right corner* represent 50 μm, respectively). *Red arrow*, positive signal in the islet. *B*, relative quantification of p65-stained positive signal in the pancreas of *db/db* mice. *C*, real-time PCR analysis of relative *il1b* mRNA expression levels in MIN6 cells with treatment of MPE or control in high-glucose (25 mmol/liter) or low-glucose (5.5 mmol/liter) medium (LG control). *D*, IL-1β protein levels in supernatant after treatment of MIN6 cells with IL-1β or IL-1β + TNFα + IFNγ. *E*, real-time PCR analysis of relative *il1b* mRNA expression levels in primary islets from HFD-induced obese mice with treatment of MPE or HG control. *F*, IL-1β protein levels in supernatant after treatment of primary islets of HFD-induced obese mice with IL-1β or IL-1β +TNFα + IFNγ. *G*, GSIS was performed to evaluate the primary islet function from C57 mice with normal chow feeding after treatment with IL-1β or IL-1β +TNFα + IFNγ in LG control and MPE groups. *H*, real-time PCR analysis of relative *il1b* mRNA expression levels were measured after treatment with IL-1β or IL-1β + TNFα + IFNγ in primary islets of C57 mice in LG control and MPE groups. Data are presented as mean ± S.E. (*error bars*) with individual data points in histograms. *, $p < 0.05$; **, $p < 0.01$.

000642, BKS.Cg-Dock7^{m}+/+Lepr^{db}/J), *db/m* mice, and female C57BL/6J mice were obtained from the CUHK Laboratory Animal Services Center and housed in a temperature-controlled room (22 °C) on a 12-h light-dark cycle with free access to food and water.

For the *db/db* mouse studies, 12-week-old female mice were used when their β-cell function started to decline (41), as judged by increasing fasting glycemia, and treated with 200 or 400 mg/kg MPE or water by oral gavage once daily for 4 weeks. Fasting blood glucose, food intake, and body weight were measured weekly.

For the HFD-induced obese mouse study, 4-week-old female C57BL/6J mice were fed with either HFD (60% kcal% fat, catalog no. D12492, Research Diets) or NCD (LabDiet Select 50IF/6F) for 10 weeks to induce insulin resistance and impaired islet function (42, 43). These mice were treated with 200 mg/kg MPE, 400 mg/kg MPE, or water as vehicle by oral gavage once daily for 4 weeks. Fasting blood glucose, food intake, and body weight were measured weekly.

After a 4-week treatment with MPE, an OGTT was performed in both *db/db* and HFD-induced obese mice after overnight fasting for 15 h. For OGTT, the mice were gavaged with 20% glucose (1 g/kg) after collection of blood at baseline (0 min). All blood samples were collected from the tail vein at 0, 15, 30, 60, and 120 min for glucose and insulin measurements. For the ITT, mice were fasted for 6 h. Blood glucose levels were measured at 0, 30, 60, and 120 min after intraperitoneal injection of recombinant human regular

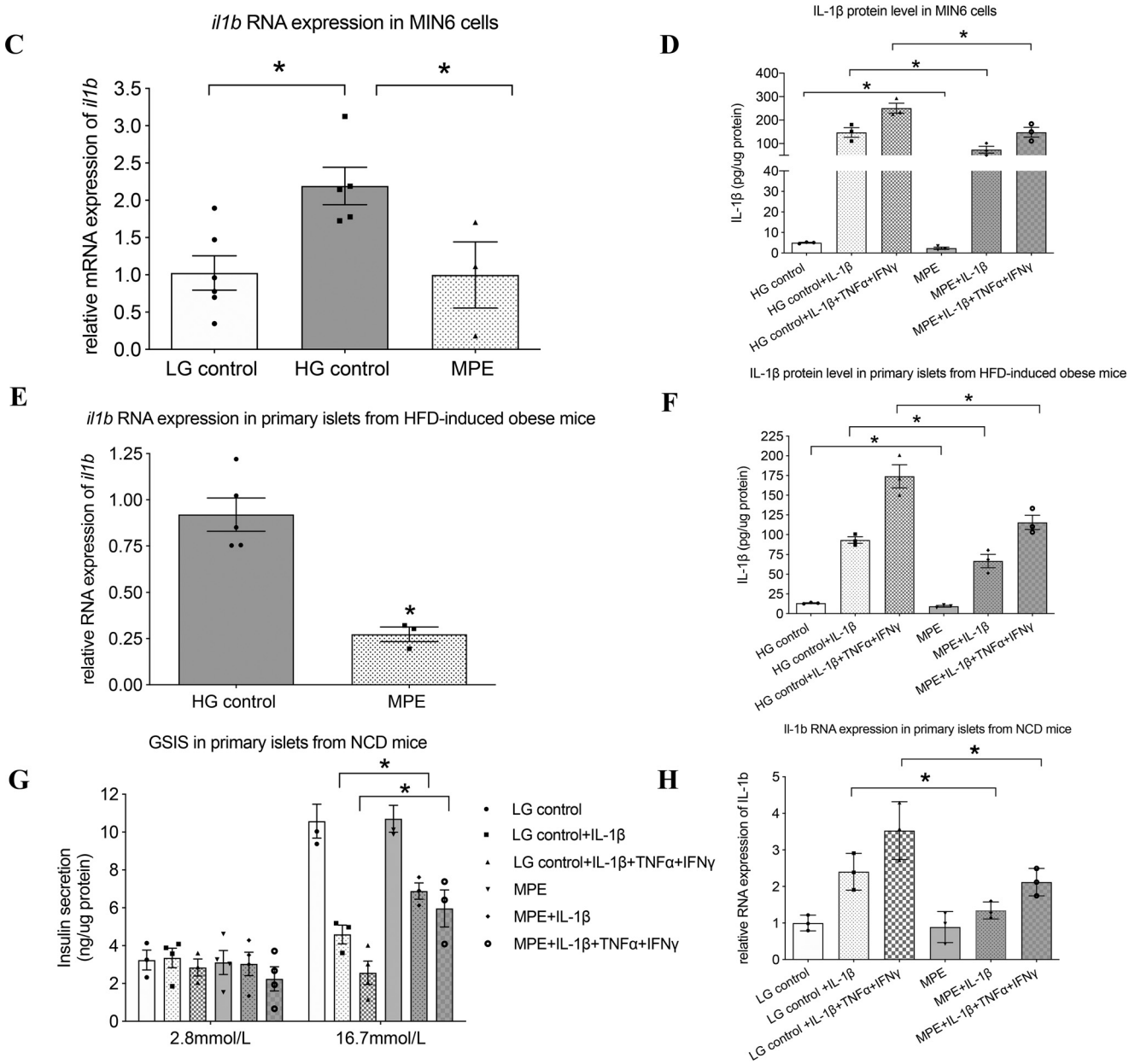

Figure 5 —*continued*

insulin (Novo Nordisk, Bagsvard, Denmark) at a dose of 0.5 IU/kg of body weight.

Histological staining

After 4 weeks of treatment with MPE or control vehicle, and following OGTT, pancreata were isolated from both *db/db* mice and HFD-induced obese mice for immunofluorescent staining of glucagon expressed in α-cells and insulin expressed in β-cells. Mouse pancreas were fixed in 4% (v/v) paraformaldehyde overnight and embedded in paraffin. Sections were cut to 4-μm thickness.

For insulin, glucagon, and IL-1β staining, after rehydration, slides of mouse pancreas were placed in 0.5% (v/v) Triton X-100 for 20 min for permeabilization, followed by 0.01 mol/liter sodium citrate buffer (pH 6.0), and heated at ~100 °C for 10 min for antigen retrieval. After blocking nonspecific antigens, guinea pig anti-insulin, rabbit anti-glucagon, or rabbit anti-IL-1β antibodies were applied to the sections overnight at 4 °C. The sections were then washed in PBST three times and incubated with fluorescence-conjugated secondary antibodies, Alexa Fluor® goat anti-guinea pig 568, and goat anti-rabbit 488 at room temperature (RT) for 1 h, followed by counterstaining of the nucleus with DAPI.

For BrdU staining, we fed *db/db* mice with freshwater daily, which contained BrdU at a concentration of 0.8 mg/ml for 7 days before mice were sacrificed. For BrdU immunohistochemistry staining, we performed the same rehydration and antigen retrieval procedures as above, followed by DNA hydrolysis by using 2 M HCl for 30 min at RT. After blocking nonspecific antigen, mouse anti-BrdU antibodies were applied to the sections overnight at 4 °C. The sections were washed by PBST three times and then incubated with

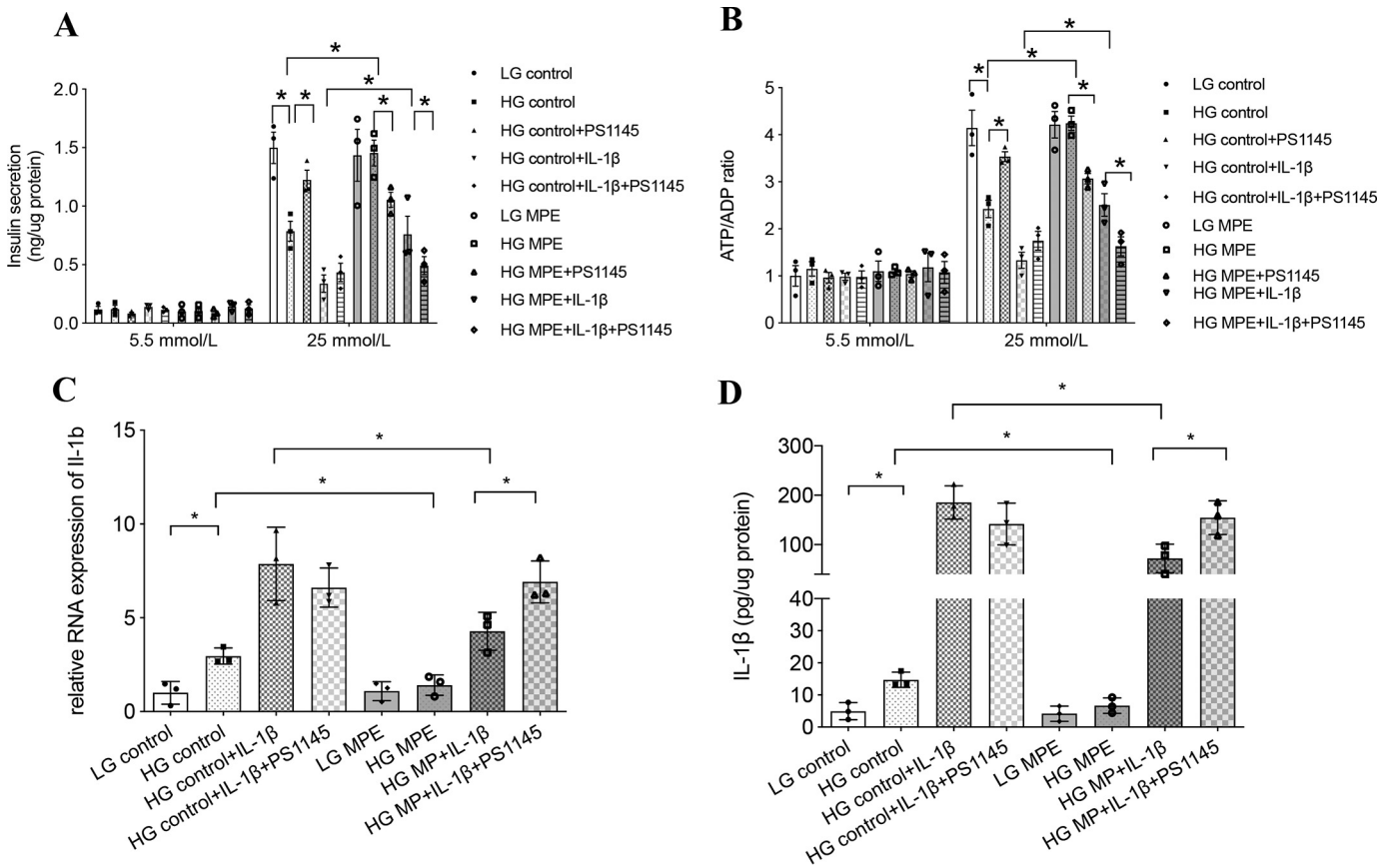

Figure 6. MPE reduces glucotoxicity and improves β-cell function by reducing inflammation in MIN6 cells. MPE attenuates IL-1β–induced inflammation in high-glucose medium, which is inhibited by IKK inhibitor (PS1145) in MIN6 cells. *A*, GSIS was performed to evaluate the anti-inflammatory effect of MPE in MIN6 cells with low-glucose or high-glucose incubation. In high-glucose incubation, MIN6 cells were divided into eight groups for treatment with control or MPE, control + PS1145 or MPE + PS1145, control + IL-1β or MPE + IL-1β, and control + IL-1β + PS1145 or MPE + IL-1β + PS1145. *B*, ATP/ADP ratio was measured in different cell groups using the same treatments as in *A*. *C*, relative RNA expression of *il1b* was measured in control or MPE, control + IL-1β or MPE + IL-1β, and control + IL-1β + PS1145 or MPE + IL-1β + PS1145. *D*, IL-1β protein levels from supernatant were measured in different cell groups using same treatments as in *C*. Data are presented as mean ± S.E. (*error bars*) with individual data points in histograms. *, $p < 0.05$.

fluorescence-conjugated secondary antibodies, Alexa Fluor® goat anti-mouse 568 at RT for 1 h, followed by counterstaining of the nucleus with DAPI.

For TUNEL analysis (Millipore), after rehydration as above, the tissue was permeabilized by protease (20 μg/ml) for 20 min, followed by inactivation of endogenous peroxidases by 3% H_2O_2 for 20 min and equilibration by TdT equilibration buffer for 30 min at RT. Afterward, the tissue was treated with TdT labeling reaction mix for 2 h at 37 °C and terminated by stop buffer. After nonspecific antigen blocking, the tissue was detected by conjugate buffer for 30 min at 37 °C. Color staining was developed by DAB for 20 min at RT, followed by counterstaining with hematoxylin (Sigma–Aldrich), dehydration, and DPX mounting.

For total p65 staining, after rehydration, slides were placed in 3% H_2O_2 for 20 min followed by 0.01 mol/liter sodium citrate buffer (pH 6.0) and heated at ~100 °C for 10 min for antigen retrieval. After blocking in 5% rabbit serum for 1 h, p65 primary antibody was applied to the sections overnight at 4 °C. The sections were washed in PBST three times and then incubated with HRP-linked secondary antibody for 1 h at RT. DAB solution (Dako) was then applied to the sections for 10 min, followed by washing with H_2O, counterstaining with hematoxylin (Sigma–Aldrich), dehydration, and DPX mounting.

For each of the five mice in the control and experimental groups (*i.e.* 20 mice in the *db/db* mice model and 20 mice in the HFD mice model), we analyzed the full pancreatic section on one slide per mouse. We used Leica Qwin image analysis software (Leica, Germany) to scan the entire pancreatic area and capture the images of individual islets within the section. We used ImageJ to measure the total pancreatic and insulin- and glucagon-positive areas (Fig. 2, *A* and *B*) and expressed the area occupied by β- and α-cells as percentages of the total pancreatic area. We then compared the mean ± S.D. of these percentage areas between control and experimental groups (Fig. 2, *C–F*). A description of the antibodies used is provided in Table S1. Positive signals of IL-1β, p65, and BrdU and positive signal in the TUNEL assay were quantified using ImageJ.

MIN6 cell culture, primary islet isolation, and treatment

The MIN6 cell line (24) (passages 20–30, courtesy of Professor Guang Ning, School of Medicine, Shanghai Jiao-Tong University, Shanghai, China) was cultured in Dulbecco's modified Eagle's medium (Invitrogen) with 15% FBS (Gibco), 1% penicillin-streptomycin (Gibco), and 50 μmol/liter 2-

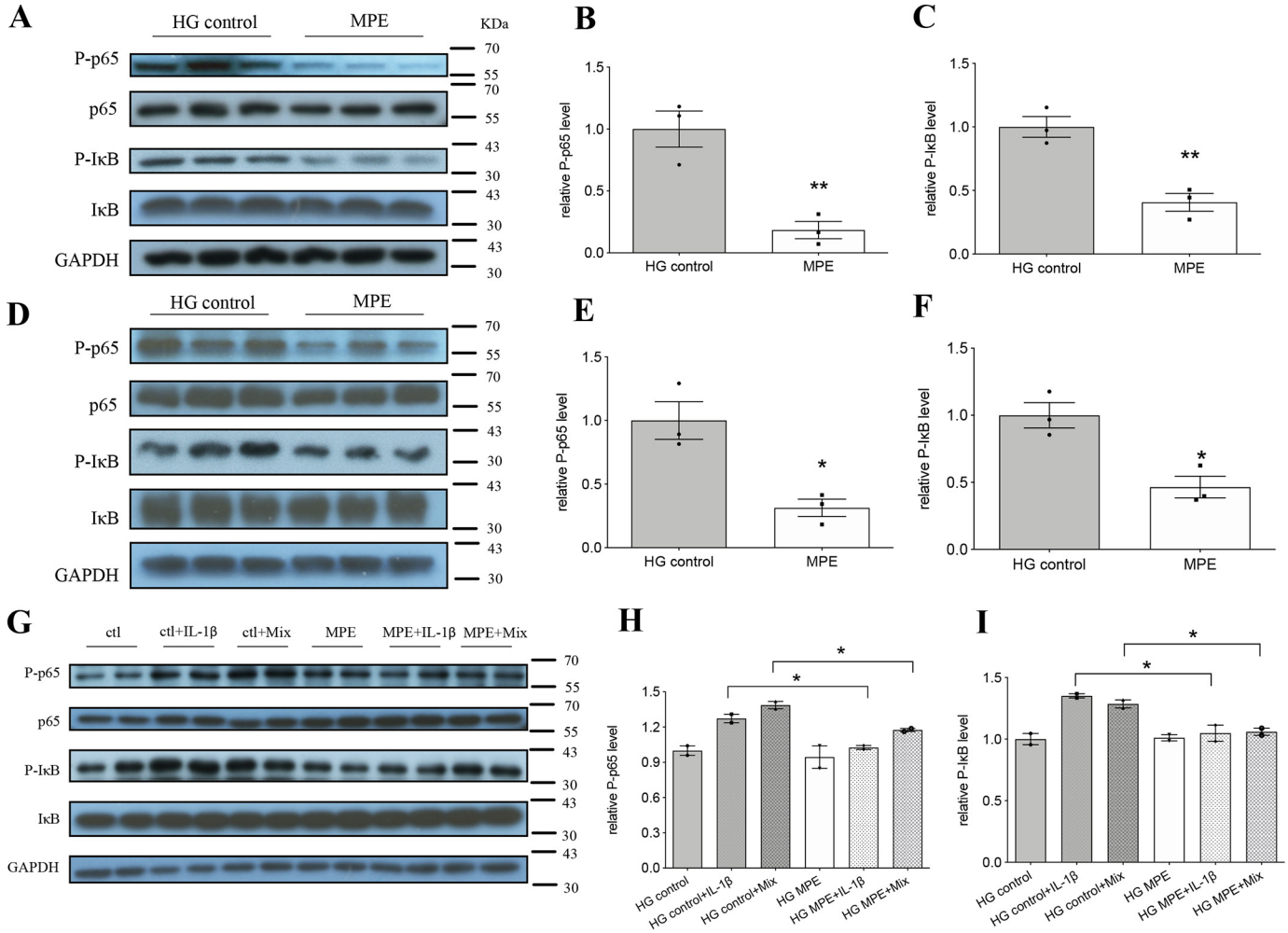

Figure 7. MPE attenuates inflammation by decreasing the protein level of NF-κB p65 and increasing the protein level of IκB. *A–C*, Western blotting analysis of respective markers in MIN6 cells. *D–F*, Western blotting analysis of respective markers in primary pancreatic islets from HFD-induced obese mice. *G–I*, Western blotting analysis of respective markers in primary pancreatic islets from C57 mice. Mix represents mixture of inflammatory cytokines (IL-1β + TNFα + IFNγ). *Ctl*, HG control. Data are presented as mean ± S.E. (*error bars*) with individual data points in histograms. *, $p < 0.05$; **, $p < 0.01$.

mercaptoethanol (Gibco). The cells were treated with MPE at concentrations of 0, 0.05, 0.5, 5, and 50 μg/ml for 24, 48, and 72 h.

Primary pancreatic islets were isolated from HFD and NCD mice as follows. Mice were anesthetized with a mixture of ketamine and xylazine (Alfasan, Holland). After clamping the duodenum ampulla, 3 ml of collagenase solution (solution G supplemented with collagenase P) (Roche Applied Science) was infused into the bile duct slowly. Solution G is composed of modified Hanks' balanced salt solution (Invitrogen) with 0.25% (w/v) BSA (Sigma). The inflated pancreas was removed and put into centrifuge tubes with 3 ml of collagenase solution before incubation at 37 °C for 10 min with gentle shaking. The digested pancreases were washed with solution G three times and filtered through a 500-μm mesh before gradient centrifugation with Histopaque 1119, 1083, and 1077 (Sigma). The uppermost layer of islets was harvested and cultured with RPMI 1640 (Gibco, catalog no. 22400) with 10% FBS and 1% penicillin-streptomycin. The islets were treated with MPE at concentrations of 0.5 μg/liter for 72 h.

Microarray analysis

Microarray analysis was performed in the laboratory of the CUHK Department of Obstetrics and Gynecology using the Agilent platform. Control and unknown RNA samples were labeled by different dyes, followed by the addition of prehybridization and reaction solutions, prepared according to the manufacturer's instructions. Thereafter, a PCR purification kit was used to combine the control and test reactions, followed by washing and eluting labeled cDNA from the column. Hybridization solution was applied to the microarray slide for further incubation at 65 °C overnight. The slides were then washed and read under an Agilent C microarray scanner.

Real-time PCR and immunoblotting

We used TRIzol (Invitrogen) to extract total RNA in MIN6 cells and primary islets from the above mouse models, followed by reverse transcription to cDNA (Takara, Japan). cDNA was applied to a SYBR Green kit (Promega) and then an Applied Biosystems 7900HT system for quantitative RT-PCR analysis. Mouse primers are shown in Table S1.

Table 1

Effects of MPE on outcome measures in various experimental models

↑, increase; ↓, decrease; (−), no change; FBG, fasting blood glucose; BW, body weight; FI, food intake; GSIS, glucose-stimulated insulin secretion; HFD, high-fat diet; IS, insulin secretion; ITT, insulin tolerance test; NCD, normal chow diet; OGTT, oral glucose tolerance test; PA, palmitate acid; WB, Western blotting.

db/db mice	HFD-induced obese mice	MIN6 cells	Primary islets from HFD-induced obese mice	Primary islets from NCD mice
↓ FBG (Fig. 1*A*); ↑ IS per week (Fig. 1*B*)	(−) FBG (Fig. 1*C*); (−) BG in OGTT (Fig. 1, *D* and *E*); ↑ IS in OGTT (Fig. 1*F*)	↑ GSIS (Fig. 3*A*); ↑ ATP/ADP ratio (Fig. 3*B*)	↑ GSIS (Fig. 3*C*); ↑ ATP/ADP ratio (Fig. 3*D*)	
↑ percentage of β-cell area (Fig. 2, *A* and *C*); (−) percentage of α-cell area (Fig. 2*B*)	↑ percentage of β-cell area (Fig. 2, *D* and *F*); (−) percentage of α-cell area (Fig. 2*E*)	↓ *pi3kca*, *pi3ckcd*, *csf2*, *nfκb1* in microarray analysis (Fig. 4, *A–J*)		
↓ p65 nuclear translocation (Fig. 5, *A* and *B*)		↓ *il1b* RNA expression (Fig. 5*C*); ↓ IL-1β protein expression with inflammatory cytokine treatment (Fig. 5*D*)	↓ IL-1β RNA expression (Fig. 5*E*); ↓ IL-1β protein expression (Fig. 5*F*)	↑ GSIS with inflammatory cytokine treatment (Fig. 5*G*); ↓ *il1b* RNA expression with inflammatory cytokine treatment (Fig. 5*H*)
(−) BW, FI (Fig. S2, *A* and *B*); (−) ITT (Fig. S2*C*); (−) OGTT (Fig. S2, *D* and *E*)	(−) BW, FI (Fig. S3, *C* and *D*); (−) ITT (Fig. S3*E*)	MPE with IKK inhibitor treatment: ↓ GSIS (Fig. 6*A*); ↓ ATP/ADP ratio (Fig. 6*B*); ↑ *il1b* RNA expression (Fig. 6*C*); ↑ IL-1β protein expression (Fig. 6*D*)		
↓ IL-1β expression in pancreas (Fig. S4, *A* and *B*)	↓ IL-1β expression in pancreas (Fig. S4, *C*, and *D*)	↓ P-p65, ↓ P-IKB by WB (Fig. 7, *A–C*)	↓ P-p65, ↓ P-IKB by WB (Fig. 7, *D–F*)	↓ P-p65, ↓ P-IKB with inflammatory cytokine treatment by WB (Fig. 7, *G–I*)
	(−) cell proliferation in pancreas (Fig. S5); (−) apoptosis by TUNEL in pancreas (Fig. S6); (−) lipid profile, GLP-1, caspase-3, glucagon, α-glucosidase activity (Fig. S7)	MPE with PA treatment: (−) GSIS (Fig. S8, *A–E*)		

Total protein from MIN6 cells or primary pancreatic islets was extracted by using ice-cold cell lysis buffer (catalog no. 9803, Cell Signaling Technology) supplemented with protease inhibitor (Roche Applied Science) and Na_3VO_4 and then adjusted to the same concentration by loading buffer and denatured. After gel electrophoresis, transfer, and blocking, membranes were incubated in the primary antibodies at 4 °C overnight. The primary antibodies included phospho-p65, p65, phospho-IκB, IκB, and GAPDH. HRP-linked anti-rabbit and anti-mouse IgG were used as secondary antibodies. Protein bands were developed by Immobilon Western Chemiluminescent HRP substrate (Millipore, Billerica, MA, USA). A description of the antibodies used is included in Table S1.

Insulin, IL-1β ELISA, and ATP/ADP ratio measurement

For measurement of mouse serum insulin, collected blood samples were put on ice for at least 30 min for clotting, followed by centrifugation at 2500 × *g* for 20 min at 4 °C. The serum was collected for measurement of insulin by ELISA (Millipore, Germany).

For GSIS study of MIN6 cells or isolated mouse islets, cells were first starved with low FBS and glucose in KRBH buffer (129 mmol/liter NaCl, 4.8 mmol/liter KCl, 1.2 mmol/liter KH_2PO_4, 1.2 mmol/liter $MgSO_4$, 2 mmol/liter $CaCl_2$, 20 mmol/liter HEPES, 24 mmol/liter $NaHCO_3$, 0.2% BSA (w/v), 0.2% FBS (w/v)) with low glucose of 5.5 mmol/liter (for MIN6 cells) or 2.8 mmol/liter (for islets). After 1 h, the medium was replaced by KRBH buffer with either low glucose (5.5 mmol/liter for MIN6 cells, 2.8 mmol/liter for islets) or high glucose (25 mmol/liter for MIN6 cells, 16.7 mmol/liter for islets) for another 2 h. The medium was collected for insulin measurement by ELISA (Millipore, Germany) according to the manufacturer's instructions, and cells were washed three times with PBS before being harvested for protein quantification (Thermo Fisher Scientific, Waltham, MA, USA).

For measurement of the IL-1β level in MIN6 cells and primary pancreatic islets, cell supernatant was collected after treatment and analyzed by IL-1β ELISA (R&D Systems) according to the manufacturer's instructions, and cells were harvested for quantification of protein content (Thermo Fisher Scientific).

For glucose-stimulated ATP/ADP ratio measurement, MIN6 cells or primary islets were starved in KRBH buffer with low glucose of 5.5 mmol (MIN6 cells) or 2.8 mmol (islets) for 1 h, followed by stimulation by KRBH buffer with high glucose of 25 mmol of glucose (MIN6 cells) or 16.7 mmol (islets) for another 2 h. The supernatant was collected for ATP/ADP ratio measurement by a bioluminescent assay kit (Abcam, UK) according to the manufacturer's instructions. Cells were harvested for measurement of protein content (Thermo Fisher Scientific).

During OGTT, mouse serum was collected for measurement of insulin by ELISA (Millipore, Germany). GSIS study of MIN6 cells or isolated mouse islets was conducted as described previously.

Cell supernatant was collected after treatment and analyzed by IL-1β ELISA (R&D Systems) and a bioluminescent ATP/ADP ratio assay kit (Abcam), respectively, according to the manufacturer's instructions, and cells were harvested for quantification of protein content.

Triglyceride, high-density lipoprotein cholesterol, GLP-1, glucagon, and caspase-3 activity measurement

After OGTT, mouse serum was collected for measurement of triglyceride (Abcam), high-density lipoprotein cholesterol (Abcam), GLP-1 (Abcam), and glucagon (Abcam) according to

the manufacturer's instructions. Caspase-3 activity (Abcam) was measured in the MIN6 cell supernatant after treatment with MPE (0.5 μg/liter) for 72 h.

Statistical analysis

In the animal experiments, all data are presented as mean ± SEM with individual data points shown in histograms. Between-group differences were compared using Student's *t* test and two-way analysis of variance with Tukey's post hoc test as appropriate. Statistical comparisons were made using Prism (GraphPad Prism 7, San Diego, CA). A p value of <0.05 was considered as statistically significant.

Data availability

Microarray data have been deposited in the Gene Expression Omnibus and are accessible through GEO accession number GSE154478. All other data are contained within the article.

Author contributions—Dandan Mao, X. Y. T., A. P. K., J. X. L., G. A. R., W. H. T., and J. C. N. C. conceptualization; Dandan Mao, X. Y. T., J. X. L., G. A. R., W. H. T., and J. C. N. C. data curation; Dandan Mao, X. Y. T., C. C. W., and C. B. S. L. formal analysis; G. A. R., W. H. T., and J. C. N. C. supervision; Dandan Mao and X. Y. T. validation; Dandan Mao, X. Y. T., Di Mao, S. W. H., C. C. W., C. B. S. L., H. M. L., C. K. W., E. C., X. M., H. C., R. C. M., P. K. C., A. P. K., J. X. L., G. A. R., W. H. T., and J. C. N. C. methodology; Dandan Mao and X. Y. T. writing-original draft; Dandan Mao and X. Y. T. project administration; Dandan Mao, X. Y. T., Di Mao, P. K. C., A. P. K., J. X. L., G. A. R., W. H. T., and J. C. N. C. writing-review and editing; H. M. L., C. K. W., and E. C. resources.

Funding and additional information—This work was supported by the HKOG Trust Fund (project code: 6903757), a CUHK Direct Grant (project code: 4054110), the CUHK Diabetes Research and Education Fund (project code: 7105545), and the CUHK Postdoctoral Fellowship Scheme. G. A. R. was supported by Wellcome Trust Senior Investigator (WT098424AIA) and Investigator (212625/Z/18/Z) awards; MRC Programme Grants MR/R022259/1, MR/J0003042/1, and MR/L020149/1; Experimental Challenge Grant DIVA, MR/L02036X/1; MRC Grant MR/N00275X/1; and Diabetes UK Grants BDA/11/0004210, BDA/15/0005275, and BDA 16/0005485.

Conflict of interest—J. C. N. C. reported receiving research grants and/or honoraria for consultancy or giving lectures from AstraZeneca, Boehringer Ingelheim, Eli Lilly, Merck Serono, Merck Sharp & Dohme, Pfizer, and Sanofi. R. C. W. M. reported receiving grants and/or honoraria for consultancy or giving lectures from AstraZeneca, Bayer, Boehringer Ingelheim, Eli Lilly, Pfizer, and Takeda. A. P. S. K. has received research grants and/or speaker honoraria from Abbott, AstraZeneca, Eli Lilly, Merck Serono, Nestle, and Novo Nordisk. E. C. reported receiving grants from Lee Powder and Sanofi. G. A. R. has received grant funding from Servier and from Sun Pharma.

Abbreviations—The abbreviations used are: T2D, type 2 diabetes; AUC, area under the curve; GLP-1, glucagon-like peptide 1; GSIS, glucose-stimulated insulin secretion; HFD, high-fat diet; IFN-γ, interferon γ; IκB, inhibitor of κB; IL-1β, interleukin-1β; ITT, insulin tolerance test; MIN6, mouse insulinoma 6 cell line; MPE, Maidong polysaccharide extract; NCD, normal chow diet; NF-κB, nuclear factor κB; OGTT, oral glucose tolerance test; p-, phosphorylated; RT, room temperature; TNFα, tumor necrosis factor α; DAB, 3,3′-diaminobenzidine; DAPI, 4′,6-diamidino-2-phenylindole; IKK, pro-inflammatory IκB kinase; p-, phosphorylated; TUNEL, terminal deoxynucleotidyltransferase-mediated dUTP nick end labeling; CUHK, Chinese University of Hong Kong; HRP, horseradish peroxidase; FBS, fetal bovine serum; WB, Western blotting.

References

1. World Health Organization (2016) Global Report on Diabetes, p. 6, World Health Organization, Geneva
2. Cho, N. H., Shaw, J. E., Karuranga, S., Huang, Y., da Rocha Fernandes, J. D., Ohlrogge, A. W., and Malanda, B. (2018) IDF Diabetes Atlas: global estimates of diabetes prevalence for 2017 and projections for 2045. *Diabetes Res. Clin. Pract.* **138,** 271–281 CrossRef Medline
3. Tahrani, A. A., Bailey, C. J., Del Prato, S., and Barnett, A. H. (2011) Management of type 2 diabetes: new and future developments in treatment. *Lancet* **378,** 182–197 CrossRef Medline
4. Kim, J. E., Hwang, I. S., Choi, S. I., Lee, H. R., Lee, Y. J., Goo, J. S., Lee, H. S., Son, H. J., Jang, M. J., Lee, S. H., Kang, B. C., and Hwang, D. Y. (2012) Aqueous extract of *Liriope platyphylla*, a traditional Chinese medicine, significantly inhibits abdominal fat accumulation and improves glucose regulation in OLETF type II diabetes model rats. *Lab. Anim. Res.* **28,** 181–191 CrossRef Medline
5. Ding, L., Li, P., Lau, C. B., Chan, Y. W., Xu, D., Fung, K. P., and Su, W. (2012) Mechanistic studies on the antidiabetic activity of a polysaccharide-rich extract of *Radix Ophiopogonis*. *Phytother. Res.* **26,** 101–105 CrossRef Medline
6. Liu, Y., Wan, L., Xiao, Z., Wang, J., Wang, Y., and Chen, J. (2013) Antidiabetic activity of polysaccharides from tuberous root of *Liriope spicata* var. *prolifera* in KKAy mice. *Evid. Based Complement. Alternat. Med.* **2013,** 349790 CrossRef Medline
7. Xu, J., Wang, Y., Xu, D. S., Ruan, K. F., Feng, Y., and Wang, S. (2011) Hypoglycemic effects of MDG-1, a polysaccharide derived from *Ophiopogon japonicas*, in the ob/ob mouse model of type 2 diabetes mellitus. *Int. J. Biol. Macromol.* **49,** 657–662 CrossRef Medline
8. Wang, L. Y., Wang, Y., Xu, D. S., Ruan, K. F., Feng, Y., and Wang, S. (2012) MDG-1, a polysaccharide from *Ophiopogon japonicus* exerts hypoglycemic effects through the PI3K/Akt pathway in a diabetic KKAy mouse model. *J. Ethnopharmacol.* **143,** 347–354 CrossRef Medline
9. Bayer, Inc. (2014) ^{Pr}GLUCOBAY^{TM} acarbose: 50 and 100 mg tablets: Product Monograph. Bayer, Inc., Mississauga, Ontario, Canada
10. Ni, Q., Wang, J., Li, E. Q., Zhao, A. B., Yu, B., Wang, M., and Huang, C. R. (2011) Study on the protective effect of the Mixture of Shengmai Powder and Danshen Decoction on the myocardium of diabetic cardiomyopathy in the rat model. *Chin. J. Integr. Med.* **17,** 116–125 CrossRef Medline
11. Yabe, D., and Seino, Y. (2016) Type 2 diabetes via beta-cell dysfunction in east Asian people. *Lancet Diabetes Endocrinol.* **4,** 2–3 CrossRef Medline
12. Cerf, M. E. (2013) Beta cell dysfunction and insulin resistance. *Front. Endocrinol. (Lausanne)* **4,** 1–10 CrossRef Medline
13. Yang, H., and Li, X. (2012) The role of fatty acid metabolism and lipotoxicity in pancreatic β-cell injury: identification of potential therapeutic targets. *Acta Pharm. Sin. B* **2,** 396–402 CrossRef
14. Flannick, J., Mercader, J. M., Fuchsberger, C., Udler, M. S., Mahajan, A., Wessel, J., Teslovich, T. M., Caulkins, L., Koesterer, R., Barajas-Olmos, F., Blackwell, T. W., Boerwinkle, E., Brody, J. A., Centeno-Cruz, F., Chen, L., *et al.* (2019) Exome sequencing of 20,791 cases of type 2 diabetes and 24,440 controls. *Nature* **570,** 71–76 CrossRef Medline
15. Maedler, K., Sergeev, P., Ris, F., Oberholzer, J., Joller-Jemelka, H. I., Spinas, G. A., Kaiser, N., Halban, P. A., and Donath, M. Y. (2017) Glucose-induced beta cell production of IL-1β contributes to glucotoxicity in human pancreatic islets. *J. Clin. Invest.* **127,** 1589–1860 CrossRef Medline

16. Cunha, D. A., Hekerman, P., Ladrière, L., Bazarra-Castro, A., Ortis, F., Wakeham, M. C., Moore, F., Rasschaert, J., Cardozo, A. K., Bellomo, E., Overbergh, L., Mathieu, C., Lupi, R., Hai, T., Herchuelz, A., *et al.* (2008) Initiation and execution of lipotoxic ER stress in pancreatic beta-cells. *J. Cell Sci.* **121,** 2308–2318 CrossRef Medline
17. Eguchi, K., and Manabe, I. (2013) Macrophages and islet inflammation in type 2 diabetes. *Diabetes Obes. Metab.* **15,** 152–158 CrossRef Medline
18. Böni-Schnetzler, M., Häuselmann, S. P., Dalmas, E., Meier, D. T., Thienel, C., Traub, S., Schulze, F., Steiger, L., Dror, E., Martin, P., Herrera, P. L., Gabay, C., and Donath, M. Y. (2018) Beta cell-specific deletion of the IL-1 receptor antagonist impairs beta cell proliferation and insulin secretion. *Cell Rep.* **22,** 1774–1786 CrossRef Medline
19. Dinarello, C. A., Simon, A., and van der Meer, J. W. (2012) Treating inflammation by blocking interleukin-1 in a broad spectrum of diseases. *Nat. Rev. Drug Discov.* **11,** 633–652 CrossRef Medline
20. Maedler, K., Sergeev, P., Ris, F., Oberholzer, J., Joller-Jemelka, H. I., Spinas, G. A., Kaiser, N., Halban, P. A., and Donath, M. Y. (2002) Glucose-induced beta cell production of IL-1beta contributes to glucotoxicity in human pancreatic islets. *J. Clin. Invest.* **110,** 851–860 CrossRef Medline
21. Sousa, S. G., Oliveira, L. A., de Aguiar Magalhães, D., de Brito, T. V., Batista, J. A., Pereira, C. M. C., de Souza Costa, M., Mazulo, J. C. R., de Carvalho Filgueiras, M., Vasconselos, D. F. P., da Silva, D. A., Barros, F. C. N., Sombra, V. G., Freitas, A. L. P., de Paula, R. C. M., *et al.* (2018) Chemical structure and anti-inflammatory effect of polysaccharide extracted from *Morinda citrifolia* Linn (Noni). *Carbohydr. Polym.* **197,** 515–523 CrossRef Medline
22. Illuri, R., Bethapudi, B., Anandakumar, S., Murugan, S., Joseph, J. A., Mundkinajeddu, D., Agarwal, A., and Chandrasekaran, C. V. (2015) Anti-inflammatory activity of polysaccharide fraction of *Curcuma longa* extract (NR-INF-02). *Antiinflamm. Antiallergy Agents Med. Chem.* **14,** 53–62 CrossRef Medline
23. Gao, C., Liu, L., Zhou, Y., Bian, Z., Wang, S., and Wang, Y. (2019) Novel drug delivery systems of Chinese medicine for the treatment of inflammatory bowel disease. *Chin. Med.* **14,** 23–40 CrossRef Medline
24. Miyazaki, J., Araki, K., Yamato, E., Ikegami, H., Asano, T., Shibasaki, Y., Oka, Y., and Yamamura, K. (1990) Establishment of a pancreatic beta cell line that retains glucose-inducible insulin secretion: special reference to expression of glucose transporter isoforms. *Endocrinology* **127,** 126–132 CrossRef Medline
25. Sidarala, V., and Kowluru, A. (2017) The regulatory roles of mitogen-activated protein kinase (MAPK) pathways in health and diabetes: lessons learned from the pancreatic beta-cell. *Recent Pat. Endocr. Metab. Immune Drug Discov.* **10,** 76–84 CrossRef Medline
26. Huang, X., Liu, G., Guo, J., and Su, Z. (2018) The PI3K/AKT pathway in obesity and type 2 diabetes. *Int. J. Biol. Sci.* **14,** 1483–1496 CrossRef Medline
27. Greten, F. R., Arkan, M. C., Bollrath, J., Hsu, L. C., Goode, J., Miething, C., Göktuna, S. I., Neuenhahn, M., Fierer, J., Paxian, S., Van Rooijen, N., Xu, Y., O'Cain, T., Jaffee, B. B., Busch, D. H., *et al.* (2007) NF-κB is a negative regulator of IL-1β secretion as revealed by genetic and pharmacological inhibition of IKKβ. *Cell* **130,** 918–931 CrossRef Medline
28. Liu, T., Zhang, L., Joo, D., and Sun, S. C. (2017) NF-κB signaling in inflammation. *Signal Transduct. Target Ther.* **2,** 1–10 CrossRef Medline
29. Ackermann, A. M., and Gannon, M. (2007) Molecular regulation of pancreatic beta-cell mass development, maintenance, and expansion. *J. Mol. Endocrinol.* **38,** 193–206 CrossRef Medline
30. Yin, J., Zhang, H., and Ye, J. (2008) Traditional Chinese medicine in treatment of metabolic syndrome. *Endocr. Metab. Immune Disord. Drug Targets* **8,** 99–111 CrossRef Medline
31. Zhao, H. L., Sui, Y., Qiao, C. F., Yip, K. Y., Leung, R. K., Tsui, S. K., Lee, H. M., Wong, H. K., Zhu, X., Siu, J. J., He, L., Guan, J., Liu, L. Z., Xu, H. X., Tong, P. C., *et al.* (2012) Sustained antidiabetic effects of a berberine-containing Chinese herbal medicine through regulation of hepatic gene expression. *Diabetes* **61,** 933–943 CrossRef Medline
32. Ko, C. H., Yi, S., Ozaki, R., Cochrane, H., Chung, H., Lau, W., Koon, C. M., Hoi, S. W., Lo, W., Cheng, K. F., Lau, C. B., Chan, W. Y., Leung, P. C., and Chan, J. C. (2014) Healing effect of a two-herb recipe (NF3) on foot ulcers in Chinese patients with diabetes: a randomized double-blind placebo-controlled study. *J. Diabetes* **6,** 323–334 CrossRef
33. Hsieh, H. Y., Chiu, P. H., and Wang, S. C. (2013) Histone modifications and traditional Chinese medicinals. *BMC Complement Altern. Med.* **13,** 115–126 CrossRef Medline
34. Lawless, M. W., O'Byrne, K. J., and Gray, S. G. (2009) Histone deacetylase inhibitors target diabetes via chromatin remodeling or as chemical chaperones? *Curr. Diabetes Rev.* **5,** 201–209 CrossRef Medline
35. Wang, P., Alvarez-Perez, J. C., Felsenfeld, D. P., Liu, H., Sivendran, S., Bender, A., Kumar, A., Sanchez, R., Scott, D. K., Garcia-Ocaña, A., and Stewart, A. F. (2015) A high-throughput chemical screen reveals that harmine-mediated inhibition of DYRK1A increases human pancreatic beta cell replication. *Nat. Med.* **21,** 383–388 CrossRef Medline
36. Cernea, S., and Dobreanu, M. (2013) Diabetes and beta cell function: from mechanisms to evaluation and clinical implications. *Biochem. Med. (Zagreb)* **23,** 266–280 CrossRef Medline
37. Jablecka, A., Bogdanski, P., Balcer, N., Cieslewicz, A., Skoluda, A., and Musialik, K. (2012) The effect of oral L-arginine supplementation on fasting glucose, HbA1c, nitric oxide and total antioxidant status in diabetic patients with atherosclerotic peripheral arterial disease of lower extremities. *Eur. Rev. Med. Pharmacol. Sci.* **16,** 342–350 Medline
38. Hankard, R. G., Haymond, M. W., and Darmaun, D. (1997) Role of glutamine as a glucose precursor in fasting humans. *Diabetes* **46,** 1535–1541 CrossRef Medline
39. Piatti, P. M., Monti, L. D., Valsecchi, G., Magni, F., Setola, E., Marchesi, F., Galli-Kienle, M., Pozza, G., and Alberti, K. G. (2001) Long-term oral L-arginine administration improves peripheral and hepatic insulin sensitivity in type 2 diabetic patients. *Diabetes Care* **24,** 875–880 CrossRef Medline
40. Nair, A. B., and Jacob, S. (2016) A simple practice guide for dose conversion between animals and human. *J. Basic Clin. Pharm.* **7,** 27–31 CrossRef Medline
41. Dalbøge, L. S., Almholt, D. L., Neerup, T. S., Vassiliadis, E., Vrang, N., Pedersen, L., Fosgerau, K., and Jelsing, J. (2013) Characterisation of age-dependent beta cell dynamics in the male db/db mice. *PLoS ONE* **8,** e82813 CrossRef Medline
42. Ahrén, B., and Scheurink, A. J. (1998) Marked hyperleptinemia after high-fat diet associated with severe glucose intolerance in mice. *Eur. J. Endocrinol.* **139,** 461–467 CrossRef Medline
43. Surwit, R. S., Feinglos, M. N., Rodin, J., Sutherland, A., Petro, A. E., Opara, E. C., Kuhn, C. M., and Rebuffe-Scrive, M. (1995) Differential effects of fat and sucrose on the development of obesity and diabetes in C57BL/6J and A/J mice. *Metabolism* **44,** 645–651 CrossRef Medline